Preparation and Properties of Epoxy/Phenol Formaldehyde Novolac/Hexakis(methoxymethyl)melamine Hybrid Resins from *In Situ* Polymerization

Xinghong Zhang, Boxuan Zhou, Xueke Sun, Guorong Qi

Key Laboratory of Macromolecular Synthesis and Functionalization (Ministry of Education), Department of Polymer Science and Engineering, Zhejiang University, Hangzhou 310027, China

Received 20 September 2007; accepted 30 July 2008
DOI 10.1002/app.29016
Published online 23 September 2008 in Wiley InterScience (www.interscience.wiley.com).

ABSTRACT: Based on the self-condensation of hexakis (methoxymethyl)melamine (HMMM), the condensation between HMMM and phenol formaldehyde novolac resin (n-PF), and the addition reaction of diglycidyl ether of biphenyl A (DGEBA) and n-PF, a homogeneous, transparent hybrid thermoset was prepared via *in situ* polymerization of DGEBA, n-PF, and HMMM. No phase separations were observed even for the DGEBA/n-PF/HMMM hybrid thermoset containing 40 wt % HMMM. These hybrid thermosets had high glass-transition temperatures (98–127°C from differential scanning calorimetry and 111–138°C from dynamic mechanical analysis), excellent thermal stability with high 5 wt % decomposition temperatures (>322°C), high char yields (>24 wt %), and improved flame retardancy with high limited oxygen indices (>28.5). The excellent overall properties of these hybrid resins may lead to their applications in high-performance "green" electronic products. © 2008 Wiley Periodicals, Inc. J Appl Polym Sci 110: 4084–4092, 2008

Key words: curing of polymers; fluorescence; resins; thermal properties

INTRODUCTION

In recent years, much effort has been devoted to developing novel halogen-free flame retardants for epoxy resins used in copper-clad laminates and semiconductor encapsulates.[1–35] Nitrogen-containing flame retardants[11–13,19–28,36] are gradually attracting more attention because they can improve the flame retardancy of materials without loss of heat resistance. Furthermore, they are regarded as environmentally friendly flame retardants with less toxicity, no dioxins, and low evolution of smoke during combustion.[2] Most additive-type nitrogen-containing flame retardants[36] are in the form of melamine salts, which have poor compatibility with epoxy resins and are harmful to the overall properties of the target materials. Covalent incorporation of nitrogen-containing structures into epoxy polymers can avoid the aforementioned problems and become a practical method for making high-performance epoxy polymers.[11–13,18–28] Some reactive nitrogen-containing flame retardants such as melamine–phenol formaldehyde novolac resins,[11,18,26] isocyanurate-containing resins,[21–24,27] oxazene-containing resins,[37] and aromatic azomethine-containing and phthalazinone-containing bisphenols[25,27,28] have been reported. The aforementioned materials have excellent thermal and flame resistance. However, their synthetic routes are complex, and the products cost a lot but have low processing capability.

The most important reactive-type nitrogen-containing flame retardants are melamine and its derivatives[36,38] because of their high nitrogen content and low cost. Hexakis(methoxymethyl)melamine (HMMM; Scheme 1), synthesized by the reaction of melamine, formaldehyde, and methanol, shows good solubility in organic solvents and reaction versatility. This has led researchers to incorporate it into epoxy polymers;[11–13] HMMM is easy to self-condense or react with compounds containing hydroxyl, amido, and carbonaxyl groups. Hsiue et al.[12] and Chiang and Ma[13] reported organic–inorganic hybrid flame-retardant epoxy resins that contained melamine and silicon via a sol–gel preparation method. However, the incorporated organic components should be soluble in a water–alcohol solution, and an appropriate organofunctional alkoxysilane is a necessity. Hybrid epoxy resins composed of bisphenol A epoxy, 4,4-diaminodiphenylmethane, and HMMM were prepared through an *in situ* polymerization process with a sol–gel technique;[11] a facial coupling agent, (3-glycidoxypropyl) trimethoxysilane, was used to increase the miscibility of the cured epoxy–amine region and the cured HMMM

Correspondence to: G. Qi (qiguorong@zju.edu.cn).
Contract grant sponsor: China Postdoctoral Science Foundation; contract grant number: 20060400339.

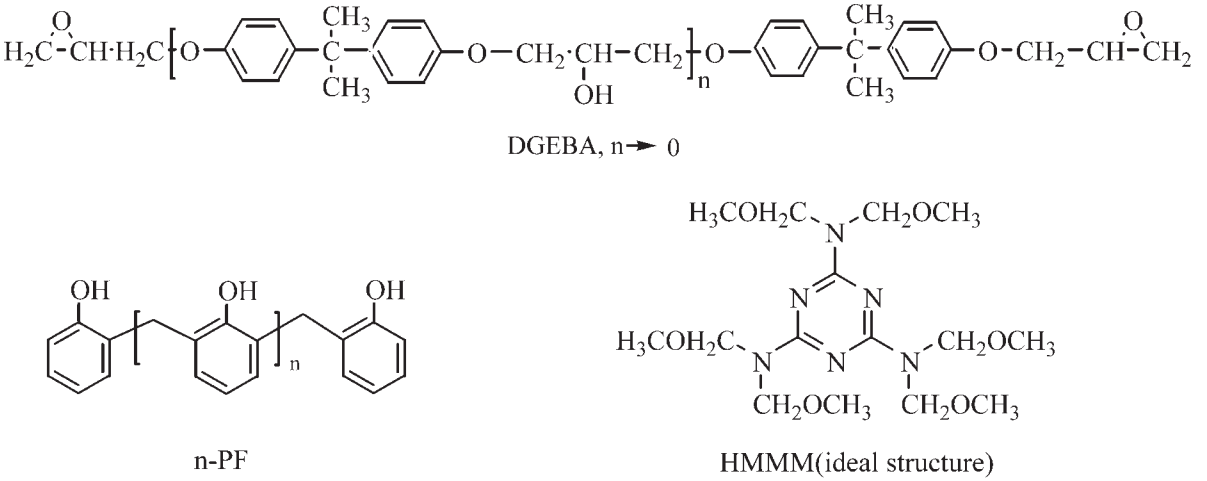

Scheme 1 Chemical structures of DGEBA, n-PF, and HMMM.

region. For an epoxy/HMMM hybrid resin, the curing process will involve at least two polymerization mechanisms (the self-condensation of HMMM and the addition reaction of an epoxy/hardener), so the structure of the resultant thermoset will mainly be decided by these mechanisms and kinetics (e.g., the rates of different reactions). Furthermore, the complete self-condensation of HMMM will ensure the improvement of the thermal stability of the resultant thermosets because some unreacted groups (e.g., $-NCH_2OCH_3$ and $-NCH_2OH$) remaining in the thermoset are not stable.

On the basis of these considerations, this work reports new epoxy hybrid resins containing diglycidyl ether of biphenyl A (DGEBA), HMMM, and phenol formaldehyde novolac resin (n-PF) that were formed via *in situ* polymerization. The thermal properties and flame retardancy of the resultant hybrid epoxy thermosets were improved dramatically.

EXPERIMENTAL

Materials

DGEBA (NPEL-127E) was kindly provided by Nan Ya Plastics (Shanghai, China) with an equivalent epoxy molecular weight of 180 g/equiv; n-PF (softening point = 85–95°C, free phenol $\leq$ 0.1 wt %) was kindly provided by KingBoard Chemical Co., Ltd. (Kunshan, China). HMMM (density = 1.2 g/mL, viscosity = 3000–6000 MPa s at 25°C, heat loss < 2 wt % at 105°C for 1.5 h, free formaldehyde $\leq$ 0.5 wt %, degree of polymerization = 1.75) was obtained from Xinhua Chemical Co. (Hangzhou, China); *p*-toluenesulfonic acid (*p*-TSA) was purchased from Sinopharm Chemical Reagent Co., Ltd. (Shanghai, China) and used as a catalyst. 4,4′-Diaminodiphenyl sulfone (DDS) was purchased from Sinopharm Chemical Reagent and used as received. Acetone was purchased from Hangzhou Shuanglin Chemical Reagent Co., Ltd (Hangzhou, China) and used as received.

Preparation of the hybrid epoxy thermosets

DGEBA/n-PF/HMMM hybrid resins with various HMMM contents were prepared by an *in situ* DGEBA/n-PF polymerization with a sol–gel process (Fig. 1). The preparation of the hybrid resin with 20 wt % HMMM is described next as an example. HMMM (12 g) and deionized water (1.2 g) were dissolved in acetone (50 mL), and the solution was stirred at room temperature. After the addition of *p*-TSA (0.12 g), the solution was stirred in an oil bath (60°C) for 1.0 h to yield homogeneous solution A. DGEBA (35.6 g) and n-PF (12.4 g) were dissolved in 50 mL of acetone, and the solution was stirred at room temperature for 1.0 h to obtain homogeneous solution B. Solutions A and B were then poured together in a beaker and stirred in an oil bath (60°C) for another 1.0 h, and then a viscous, homogeneous solution was obtained for the evaporation of acetone. This solution was then poured onto a stainless plate and treated at 60°C *in vacuo* for the complete removal of all volatiles. The obtained hybrid resin was transparent. All the epoxy thermosets were prepared with the curing procedure of 120°C for 2.0 h, 150°C for 2 h, and 180°C for 2 h.

Instrumentation

The uncured epoxy hybrid resin was coated onto a KBr pellet evenly and set in a heating cell controlled with an Omron E5T controller. The sample was heated form room temperature to 300°C at a heating rate of 20°C/min, and the real-time IR spectra were recorded with a Vector 22 Fourier transform infrared spectrophotometer (1 spectrum/30 s). The uncured epoxy hybrid resins (3.5–4.5 mg) were placed in

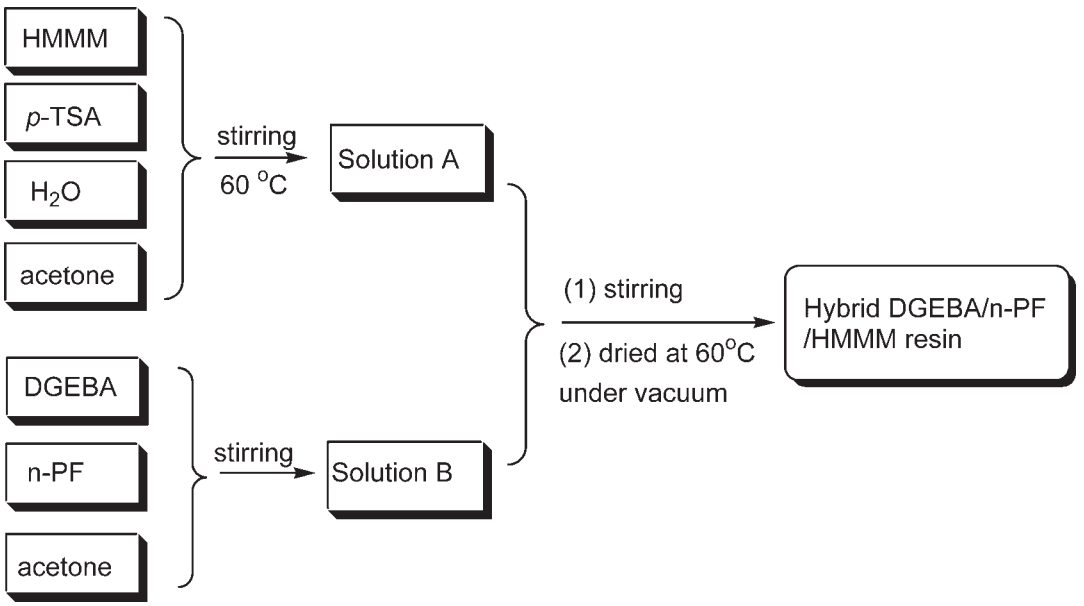

Figure 1 Preparation route of the DGEBA/n-PF/HMMM hybrid resin.

aluminum differential scanning calorimetry (DSC) pans and run on a PerkinElmer DSC 7 thermal analyzer at a heating rate of 10°C/min under an N_2 atmosphere. Glass-transition temperature (T_g) data for the hybrid thermosets were obtained from DSC measurements at a heating rate of 20°C/min under an N_2 atmosphere. Thermogravimetric analyses (TGAs) were carried out on a PerkinElmer Pyris 1 under an N_2 atmosphere at a heating rate of 10°C/min from 50 to 850°C. A specimen 40.0 mm long, 10.0 mm wide, and approximately 3.0 mm thick was used for dynamic mechanical analysis (DMA) with a PerkinElmer 7 dynamic mechanical analyzer. The storage modulus and loss tangent were determined while the sample was subjected to the temperature scan mode at a programmed heating rate of 3°C/min from room temperature to about 300°C at a frequency of 1 Hz. T_g data were also obtained from the measurement of the loss tangent peaks. Scanning electron microscopy (SEM) micrographs were taken with a JEOL JSM 840A SEM instrument (JEOL Ltd., Japan). Limited oxygen index (LOI) values were measured on an HC-2 LOI tester (Jiangning Instrument Co. Ltd., Nanjing, China) according to ASTM D 2863-77. The percentage in the O_2–N_2 mixture deemed sufficient to sustain the flame was taken as the LOI.

RESULTS AND DISCUSSION

Curing behaviors of the DGEBA/n-PF/HMMM hybrid resins

For the epoxy hybrid resins containing HMMM resin, the competition of the HMMM condensation and the epoxy/hardener reaction is the main factor determining the structure and properties of the target polymer. To avoid serious phase separation between the HMMM network and epoxy network, it is better to produce some strong interlinkages directly between the two networks at a molecular level and control the formation rate of the two networks. Herein, novolac phenol formaldehyde resin (n-PF) was chosen because the hydroxyl group of n-PF has strong reactivity with HMMM and hydrated HMMM,[39,40] and n-PF is also a hardener for preparing high-performance epoxy polymers. By real-time IR scanning of the HMMM/n-PF mixture (weight ratio = 2 : 3, curve 3, Fig. 2), which was heated at a rate of 20°C/min from room temperature to about 300°C, it was found that IR peaks at 1084 and 912

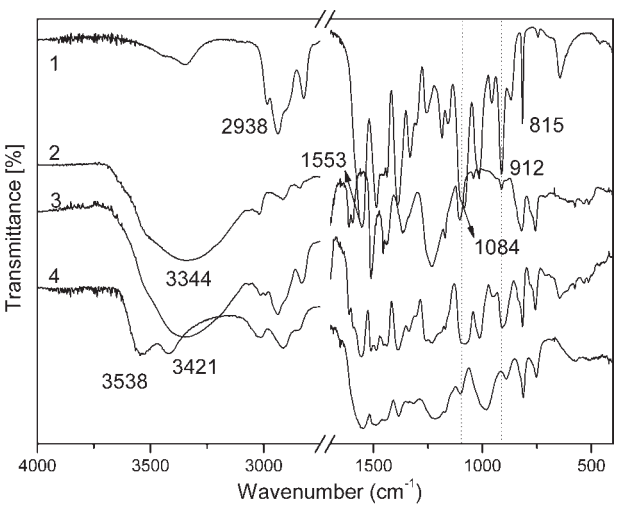

Figure 2 IR spectra of (1) HMMM, (2) n-PF, (3) HMMM (40%)/n-PF, and (4) HMMM (40%)/n-PF thermoset.

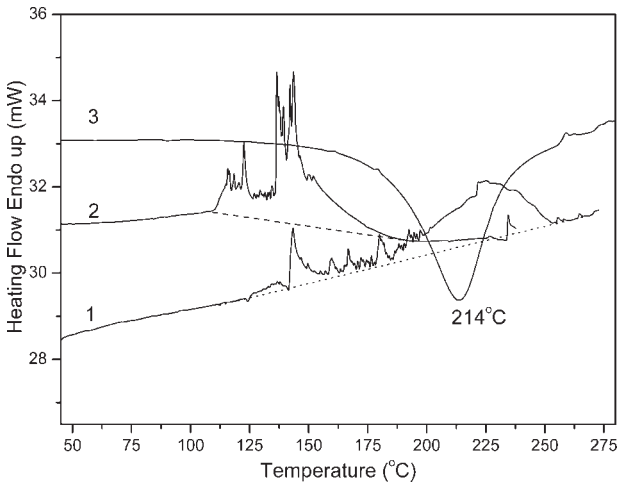

Figure 3 DSC curves of (1) HMMM (40 wt %)/n-PF without *p*-TSA, (2) HMMM (40 wt %)/n-PF/*p*-TSA (1.0 wt % of the weight of HMMM), and (3) DGEBA/n-PF (equal molar ratio) at a heating rate of 10°C/min under N_2.

cm^{-1}, which were the characteristic vibration peaks of —OCH_3 of HMMM, disappeared after curing, and the wide absorption peak (3344 cm^{-1}) of the phenolic hydroxyl group of the HMMM/n-PF mixture decreased and shifted to higher wave numbers (3538 and 3421 cm^{-1}; curve 4, Fig. 2). The disappearance of both groups in real-time IR scanning spectra showed that the reaction of the hydroxyl group of n-PF and —OCH_3 of HMMM occurred and that a new chemical bond (—NCH_2OAr) was produced. For further understanding of the reactions related to these hybrid resins, the reaction behaviors of the n-PF/HMMM mixture, the DGEBA/n-PF mixture, and the DGEBA/n-PF/HMMM hybrid resins were evaluated by DSC in detail.

Figure 3 shows the DSC thermograms of the n-PF/HMMM mixtures (with and without *p*-TSA) and DGEBA/n-PF mixture. Irregular endothermic peaks were observed from the DSC curves of the n-PF/HMMM mixture (curves 1 and 2) because the condensations (self-condensation of HMMM and condensation between HMMM and n-PF) were very fast reactions along with the mass loss resulting from the release of small molecules such as H_2O, CH_3OH, and CH_2O.[39–41] The self-condensation of pure HMMM could not occur even with heating to 220°C. If the epoxy network formed in advance of the HMMM network or at the same time as the HMMM network, the former network would retard the complete curing of HMMM, and so these small molecules could not be released completely or in a timely fashion. They might be released at high temperatures, and small bubbles would be generated in the thermoset and result in the deterioration of the mechanical and thermal properties of the resultant thermoset. That is, it is necessary for the HMMM condensation to occur in advance. Thus, it is better to ensure that the onset reaction temperature of the epoxy/hardener is higher than that of the HMMM condensation or that the reaction rate of the epoxy/hardener is lower than that of the HMMM condensation. Figure 3 shows that the onset reaction temperature of the DGEBA/n-PF mixture was about 170°C and met these requirements. Furthermore, *p*-TSA could accelerate the condensation of the n-PF/HMMM mixture effectively. It is practical that the rate of condensation of HMMM (or the n-PF/HMMM mixture) could be adjusted by the alteration of the amounts of *p*-TSA.

Figure 4 shows the DSC curves of the DGEBA/n-PF/HMMM (20 wt %) hybrid resins with different amounts of *p*-TSA. The exothermal temperature at which the maximum conversion rate occurred in the DSC curve (T_p) increased with increasing amounts of *p*-TSA. This indicates that more *p*-TSA favored the rapid formation of the HMMM network, which could retard the curing reaction of DGEBA/n-PF dramatically. From our experimental results, 1.0–2.0 wt % *p*-TSA in the hybrid resin was suitable for making the target polymers with improved properties.

It is important for the weight ratio of each component to have a strong influence on the curing behavior of the hybrid resin. From Figure 5, we can see that all hybrid resins had unsymmetrical DSC curves and that T_p increased from 186 to 200°C with the HMMM content increasing from 5 to 40 wt %. This indicates that each hybrid resin had different enthalpy changes during curing. Because the condensation of HMMM (and n-PF) in the presence of *p*-TSA was faster than the reaction of the DGEBA/n-PF

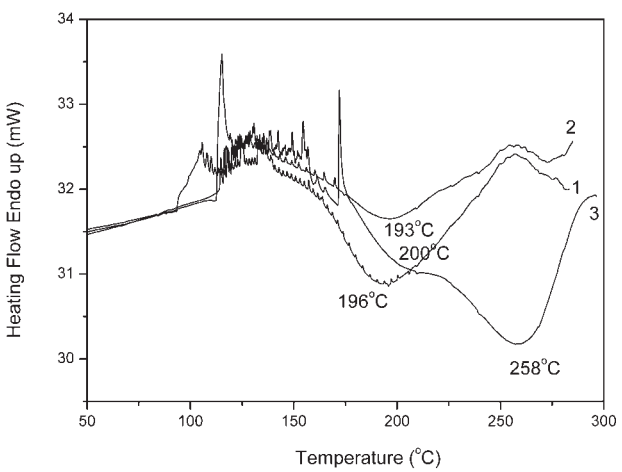

Figure 4 DSC curves of the DGEBA/n-PF/HMMM (20 wt %) hybrid resin with different amounts of *p*-TSA (10°C/min, N_2): (1) 1.0, (2) 2.0, and (3) 3.0 wt % of HMMM.

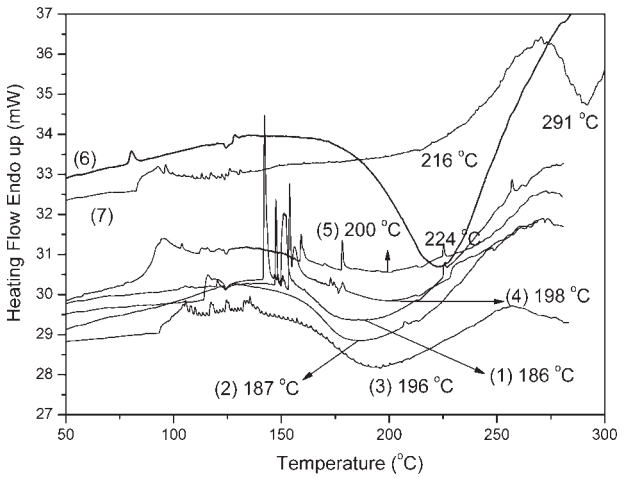

Figure 5 DSC curves of various hybrid resins (*p*-TSA: 1.0 wt % of HMMM) with different HMMM contents (10°C/min, N_2): (1) DGEBA/n-PF/HMMM (5 wt %), (2) DGEBA/n-PF/HMMM (10 wt %), (3) DGEBA/n-PF/HMMM (20 wt %), (4) DGEBA/n-PF/HMMM (30 wt %), (5) DGEBA/n-PF/HMMM (40 wt %), (6) DGEBA/DDS (equal molar ratio), and (7) DGEBA /DDS/HMMM (20 wt %).

mixture, the formed HMMM network with some fixed n-PF retarded the next curing reaction of DGEBA/n-PF. The greater the HMMM content in the hybrid resins was, the more the curing reaction of DGEBA/n-PF was retarded. Thus, introducing more HMMM into the epoxy resin may result in an imperfect structure of the resultant hybrid thermoset.

Figure 6 presents schematic cartoons illustrating the curing process of the DGEBA/n-PF/HMMM hybrid resin in light of the aforementioned DSC analyses. The HMMM (and n-PF) network would be formed first with the elevation of the temperature. The HMMM network would be linked to many hydroxyl groups, like nets immersed in the sea of the epoxy monomers and hardeners [Fig. 6(B)]. Extending the curing time of this stage would favor the release of more small molecules and strengthen the thermal properties of the target polymers. Herein, the HMMM network linked with n-PF could be regarded as a macromolecular hardener that was *in situ* produced and could react with DGEBA continuously. Thus, the direct linkages between the two networks were built with an increase in the temperature (from B to C in Fig. 6). In this stage, the epoxy network was formed and certainly linked with the HMMM network. Further cure (postcure) of the stage [Fig. 6(C)] made both networks tightly integrated [Fig. 6(D)]. Through the aforementioned curing, the target hybrid thermosets showed excellent overall properties, which are discussed next in detail.

The transparent DGEBA/n-PF/HMMM hybrid thermosets, 80.0 mm long, 10.0 mm wide, and 3.0–4.0 mm thick, could be obtained without any bubbles (Fig. 7) even when 40 wt % HMMM was used in the formula. Its fracture surface was very smooth, and no obvious phase separation appeared in an SEM photograph [Fig. 8(A)]. To understand the influence of the formation rate of the HMMM network and the epoxy network on the morphology of the resultant hybrid thermoset, the DGEBA/DDS/HMMM (20 wt %) hybrid resin was prepared. The curing reaction of DGEBA/DDS (curve 6, Fig. 5) in this system was retarded dramatically by the HMMM network formed in advance because of the poor reactivity of DDS with DGEBA (curve 7, Fig. 5). This meant that the corresponding epoxy region

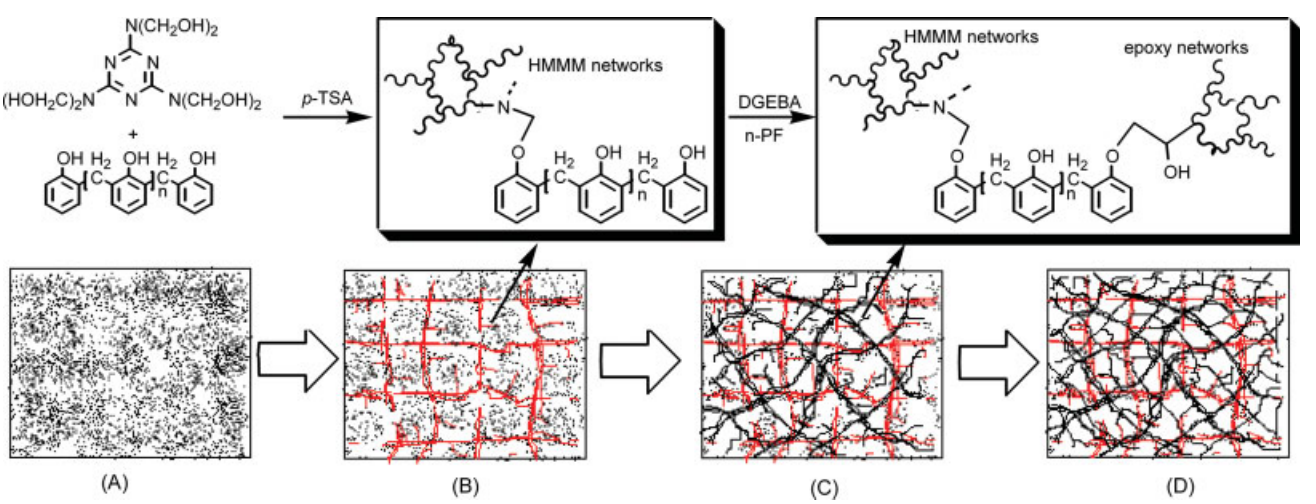

Figure 6 Schematic cartoons illustrating the cure process of the DGEBA/n-PF/HMMM hybrid resins: (A) the DGEBA/n-PF/HMMM mixture before cure, (B) the HMMM and HMMM/n-PF networks that formed, (C) the epoxy networks that formed, and (D) both networks buttoned tightly by postcuring. [Color figure can be viewed in the online issue, which is available at www.interscience.wiley.com.]

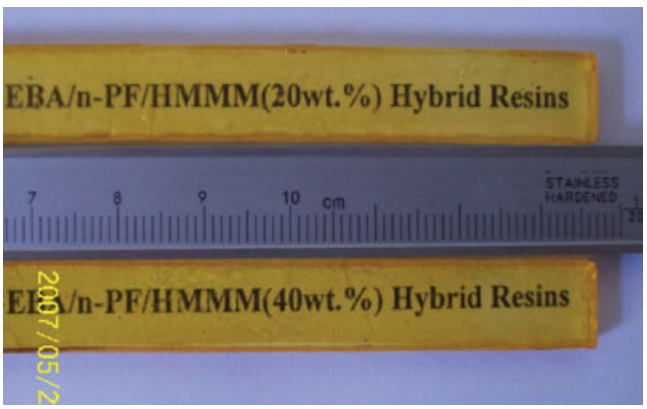

Figure 7 Digital photograph of the DGEBA/n-PF/HMMM hybrid thermosets with 20 and 40 wt % HMMM (*p*-TSA: 1.0 wt % of HMMM; curing conditions: 120°C for 2.0 h, 150°C for 2 h, and 180°C for 2 h). [Color figure can be viewed in the online issue, which is available at www.interscience.wiley.com.]

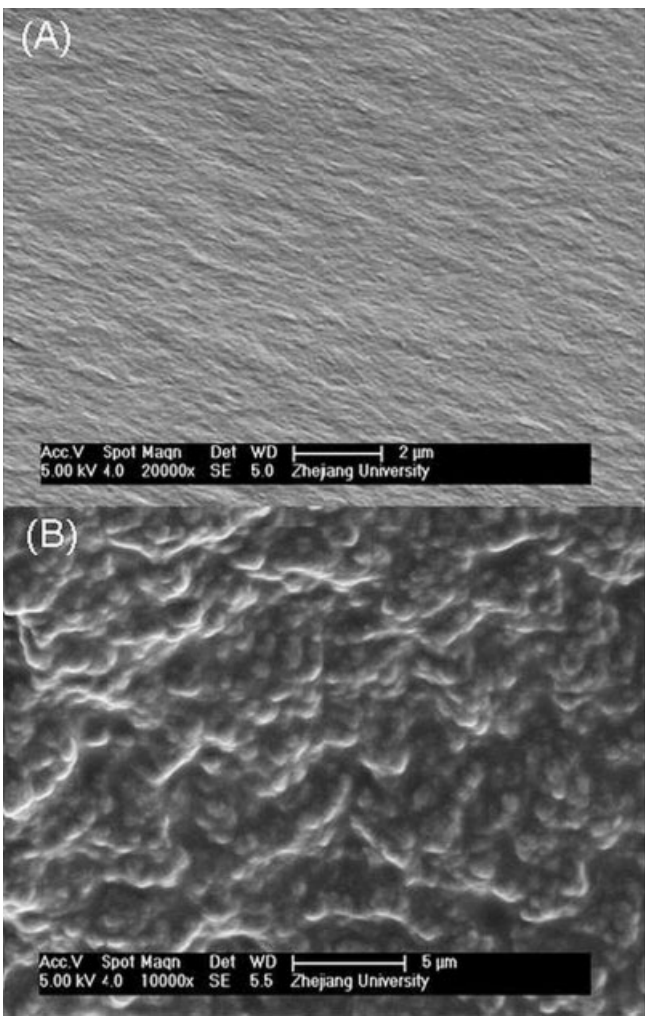

Figure 8 SEM micrographs of the fractured surfaces of (A) DGEBA/n-PF/HMMM (40 wt %) cured at 120°C for 2.0 h, 150°C for 2 h, and 180°C for 2 h and (B) DGEBA/DDS/HMMM (20 wt %) cured at 120°C for 2 h, 180°C for 2 h, and 200°C for 2 h (*p*-TSA: 1.0 wt % of HMMM).

could not cure completely even if a postcuring process was performed. The DGEBA/DDS/HMMM (20 wt %) hybrid thermoset was opaque, and its fracture surface [Fig. 8(B)] was very rough and showed serious phase separation with a domain size of approximately 1 μm.

Thermal properties and flame retardancy of the DGEBA/n-PF/HMMM hybrid thermosets

The T_g values of these hybrid thermosets with different HMMM contents were evaluated by DSC and are shown in Figure 9. Stevens and Richardson[42] reported that T_g of the cured HMMM resin was not detectable via DSC because of its high crosslink density.[42] Here, a heat capacity transition (beyond 150°C; curve 7, Fig. 9) was observed when it was heated from 40 to 220°C. It was observed that the T_g values of the hybrid thermosets containing 5, 10, 20, 30, and 40 wt % HMMM were 98, 106, 120, 125, and 127°C (curves 2–6), respectively, and higher than that of the DGEBA/n-PF thermoset (90°C; curve 1, Fig. 9). Because of the two-sided role of n-PF in the curing process, the epoxy network and HMMM network were "buttoned" together tightly in the late curing stage. Thus, some of the rigid triazine moieties, which were relatively difficult for free rotation and vibration, were copolymerized with DGEBA and n-PF. Furthermore, the chain motion of the DGEBA/n-PF network was also inhibited by the HMMM network (and HMMM/n-PF network) formed in advance. These factors increased the T_g values of these hybrid thermosets. Here, only one T_g was observed for all the hybrid thermosets, and this indicated no phase separations.

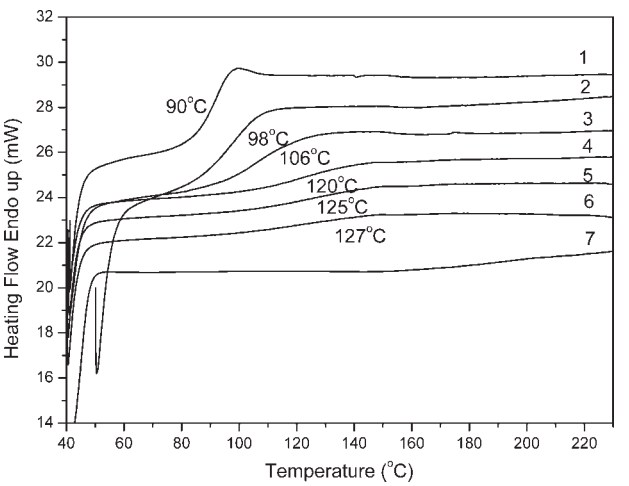

Figure 9 Second-scan DSC curves of the DGEBA/n-PF/HMMM hybrid thermosets (20°C/min, N_2): (1) DGEBA/n-PF (no HMMM added), (2) 5 wt % HMMM, (3) 10 wt % HMMM, (4) 20 wt % HMMM, (5) 30 wt % HMMM, (6) 40 wt % HMMM, and (7) the HMMM thermoset.

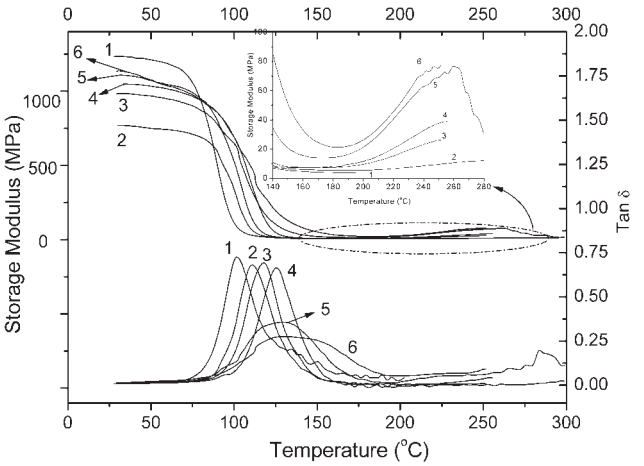

Figure 10 DMA curves of the DGEBA/n-PF/HMMM hybrid thermosets with the curing procedure of 120°C for 2 h, 150°C for 2 h, and 180°C for 2 h (3°C/min, frequency = 1 Hz): (1) 0, (2) 5, (3) 10, (4) 20, (5) 30, and (6) 40 wt % HMMM.

DMA can provide more specific information about the microstructure and thermomechanical properties of epoxy thermosets. Figure 10 shows the dynamic mechanical behaviors of the hybrid thermosets with various HMMM contents at a heating rate of 3°C/min with a frequency of 1 Hz. The initial storage modulus at 50°C of these hybrid thermosets increased from about 750 to 1072 MPa with the increase in the HMMM content, whereas it was lower than that of the DGEBA/n-PF thermoset (1210 MPa; curve 1, Fig. 10) with a postcuring stage at 220°C for 2 h (note that the DGEBA/n-PF thermoset with the procedure of 120°C for 2.0 h, 150°C for 2 h, and 180°C for 2 h was too brittle to test by DMA). That is, the incorporation of the rigid triazine moiety into the epoxy network could strengthen the mechanical properties of the resultant hybrid thermoset. Moreover, the crosslink density of the hybrid thermosets was improved with increasing HMMM content, and this was supported by their T_g values. However, the ultimate storage modulus of these hybrid thermosets increased slightly with increasing HMMM content at high temperatures (beyond 200°C; see Fig. 10) because incorporating more HMMM into the epoxy network could reduce the curing extent of the target thermosets prepared under the same curing conditions.

Herein, only one loss tangent peak was observed for each hybrid thermoset, and the T_g values (peak temperatures of the α-relaxation transition at 1 Hz; see Table I) of the hybrid thermosets with 5, 10, 20, 30, and 40 wt % HMMM were 111, 118, 125, 129, and 138°C, respectively, and higher than that of the DGEBA/n-PF thermoset (102°C) with a postcuring stage. The corresponding heights of the loss tangents of these hybrid thermosets were 0.68, 0.69, 0.66, 0.36, and 0.28, respectively. When the HMMM content was less than 20 wt %, the shapes of the loss tangent peaks and the heights of the loss tangents were almost the same (0.68–0.66) and close to those of the DGEBA/n-PF thermoset (0.73). This indicates that the microstructure of the hybrid thermoset with 5, 10, and 20 wt % HMMM had no marked changes in comparison with the DGEBA/n-PF thermoset. When the HMMM contents were 30 and 40 wt %, the corresponding loss tangent became wider and lower. This means that the uniformity of the microstructure of both hybrid thermosets was not as good as that of the hybrid thermosets with 5–20 wt % HMMM. However, no phase separation could be observed from an SEM image of the hybrid thermoset with 40 wt % HMMM [Fig. 8(A)].

The thermal stability and thermal degradation patterns of the DGEBA/n-PF/HMMM hybrid thermosets were revealed by TGA. Figures 11 and 12 show

TABLE I
Thermal Stability Parameters for the DGEBA/n-PF/HMMM Hybrid Thermosets

HMMM content (wt %)	T_g (°C)				Char yield at 850°C (wt %)				
	DSC	DMA	$T_{d,5\%}$ (°C)[a]	T_{max}[a]		A*[b]	K*[b]	IPDT (°C)[b]	LOI
0	90	102	413	460.9	14.73	0.60	1.32	687.9	21.5
5	98	111	384	453.1	24.14	0.65	1.59	873.0	28.5
10	106	118	356	451.5	28.84	0.66	1.79	985.8	32.4
20	120	125	332	445.2	32.72	0.68	1.94	1097.3	35.8
30	125	129	322	431.9	33.68	0.67	2.02	1127.0	37.0
40	127	138	322	425.6	35.20	0.67	2.10	1164.4	38.7
HMMM thermoset	—	—	285	405.2	14.47	0.57	1.34	664.4	—[c]

[a] $T_{d,5\%}$ indicates the apparent thermal stability of the epoxy thermosets; T_{max} indicates the maximum decomposition temperature of the epoxy thermosets.

[b] IPDT, proposed early on by Doyle,[43] can be discussed in a quantitative thermal analysis containing the char residue of the resulting thermosets at a high temperature. From the TGA results, IPDT can be calculated with the following equation: IPDT (°C) = $A^*K^*(T_f - T_i) + T_i$, where A^* is the area ratio of the total experimental curve divided by the total TGA thermogram, K^* is the coefficient of A^*, and T_i and T_f are the initial and final experimental temperatures, respectively.

[c] The LOI value could not be measured because the cured sample could not be obtained.

the TGA curves and first-derivative curves of all the thermosets, respectively. The corresponding thermal parameters [5 wt % decomposition temperature ($T_{d,5\%}$), char yield, and integral procedure decomposition temperature (IPDT)[43]] of these thermosets are collected in Table I. $T_{d,5\%}$ of the HMMM thermoset was 285°C, although the triazine structure has been reported to be a highly thermally stable structure.[11,18,26] This may be attributed to the decomposition of the weak crosslinking points between the triazine ring and some unreacted groups (e.g., $-NCH_2OCH_3$, $-NCH_2OH$, and $-NCH_2OCH_2N-$) in the HMMM thermoset. For the hybrid resins, the probability of producing the weak linkages and unreacted groups was decreased because n-PF could react with HMMM, and a heat-resistant $-NCH_2OAr$ linkage in the matrix was produced. It can be seen from Figure 11 that all $T_{d,5\%}$ values of the hybrid thermosets were higher ($T_{d,5\%}$ = 322–384°C) than that of the HMMM thermoset. Furthermore, the one-stage weight-loss behavior (Fig. 12) was observed for all hybrid thermosets and the DGEBA/n-PF thermoset during heating in an N_2 atmosphere. This also demonstrated that each hybrid thermoset had one domain.

The high-temperature thermal stability of the hybrid thermosets was also improved significantly. The char yields (850°C) of the HMMM thermoset and the DGEBA/n-PF thermoset were 14.47 and 14.73 wt %, respectively (curves 1 and 7, Fig. 11). Correspondingly, their IPDT values, which indexed a quantitative evaluation for the resulting thermosets at a high temperature,[44] were very low (Table I). However, the incorporation of HMMM into the DGEBA/n-PF network showed a significant effect on improving the high-temperature thermal stability, resulting in a retarded weight-loss rate (curves 2–6, Fig. 12), improved char residue (24.14–35.20), and IPDT values (873.0–1164.4; Table I). This effect was also observed to be more significant for the hybrid thermosets with higher HMMM contents. The high char yields of these hybrid thermosets implied that there were fewer volatiles being released from the thermosets during heating. Fewer volatiles released from the hybrid thermosets might imply poor flammability.

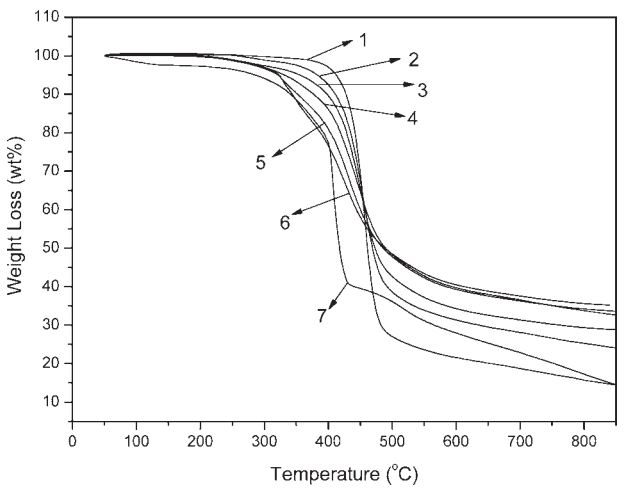

Figure 11 TGA curves of the DGEBA/n-PF/HMMM hybrid thermosets (10°C/min, N_2): (1) 0, (2) 5, (3) 10, (4) 20, (5) 30, and (6) 40 wt % HMMM and (7) HMMM thermosets.

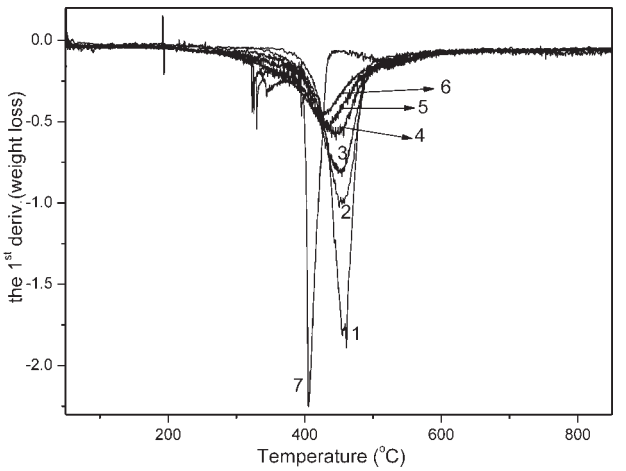

Figure 12 First-derivative curves of the DGEBA/n-PF/HMMM hybrid thermosets (10°C/min, N_2): (1) 0, (2) 5, (3) 10, (4) 20, (5) 30, and (6) 40 wt % HMMM and (7) HMMM thermosets.

LOI measures the minimum oxygen concentration (in a flowing mixture of oxygen–nitrogen gas) required to support candlelike downward flame combustion.[2] A material with an LOI of 26 or higher is rated as a flame-retardant material. It is strongly dependent on the char residue for halogen-free polymers[43] and is suitable as a semiqualitative indicator of the effectiveness of flame retardants in a laboratory. The flammability of the hybrid thermosets was evaluated with their LOIs (Table I). The improvement of HMMM with respect to the nonflammability of the hybrid epoxy thermoset was remarkable, as the LOI value was leveled up from 28.5 to 38.7 when the HMMM content was increased from 5 to 40 wt %. The high LOI values of the hybrid thermosets indicated that they could be used as halogen-free flame-retardant materials.

CONCLUSIONS

New hybrid epoxy resins composed of DGEBA, n-PF, and HMMM were prepared through an *in situ* polymerization process. The resultant hybrid thermosets were transparent and showed no phase separation in DSC and DMA results. Because of the reactions of n-PF with HMMM and DGEBA, the T_g values, $T_{d,5\%}$ values, and thermomechanical properties of the hybrid thermosets were all enhanced

compared with those of the DGEBA/n-PF thermoset. The weight-loss rates of the hybrid thermosets were retarded dramatically with the incorporation of HMMM, and this resulted in high char yields at high temperatures and excellent inherent thermal stability. The nonflammability of the cured hybrid epoxy resins was also significantly improved with a high LOI value beyond 28.5. These hybrid materials may be attractive for use in high-performance "green" electronic products because of their outstanding properties and absence of a halogen element.

References

1. Bergendahl, C. B. Alternatives to Halogenated Flame Retardants in Electronic and Electrical Products; IVF Research Publication 99824; IVF: Molndal, Sweden, 1999.
2. Lu, S. Y.; Hamerton, I. Prog Polym Sci 2002, 27, 1661.
3. Liu, Y. L. J Polym Sci Part A: Polym Chem 2002, 40, 359.
4. Liu, Y. L.; Wu, C. S.; Chiu, Y. S.; Ho, W. H. J Polym Sci Part A: Polym Chem 2003, 41, 2354.
5. Chiu, Y. S.; Liu, Y. L.; Wei, W. L.; Chen, W. Y. J Polym Sci Part A: Polym Chem 2003, 41, 432.
6. Liu, Y. L.; Hsiue, G. H.; Chiu, Y. S. J Polym Sci Part A: Polym Chem 1997, 35, 565.
7. Liu, Y. L.; Tsai, S. H. Polymer 2002, 43, 5757.
8. Liu, Y. L.; Wu, C. S.; Hsu, K. Y.; Chang, T. C. J Polym Sci Part A: Polym Chem 2002, 40, 2329.
9. Liu, Y. L.; Wu, C. S.; Chiu, Y. S.; Ho, W. S. J Polym Sci Part A: Polym Chem 2003, 41, 235.
10. Liu, Y. L.; Chen, Y. J. Polymer 2004, 45, 1797.
11. Wu, C. S.; Liu, Y. L. J Polym Sci Part A: Polym Chem 2004, 42, 1868.
12. Hsiue, G. H.; Liu, Y. L.; Liao, H. H. J Polym Sci Part A: Polym Chem 2001, 39, 986.
13. Chiang, C. L.; Ma, C. C. M. Eur Polym J 2002, 38, 2219.
14. Wu, C. S.; Liu, Y. L.; Chiu, Y. S. Polymer 2002, 43, 1773.
15. Wang, C. S.; Lin, C. H. Polymer 1999, 40, 747.
16. Wang, C. S.; Lin, C. H. J Polym Sci Part A: Polym Chem 1999, 37, 3903.
17. Lin, C. H.; Wang, C. S. J Polym Sci Part A: Polym Chem 2000, 38, 2260.
18. Shieh, J. Y.; Wang, C. S. Polymer 2001, 42, 7617.
19. Lin, C. H.; Wang, C. S. Polymer 2001, 42, 1869.
20. Tarek, A.; Hajime, T.; Tsutomu, T. Polymer 2004, 45, 7903.
21. Von, G. W.; Huber, J.; Kapitza, H.; Rogler, W. J Vinyl Addit Technol 1997, 3, 175.
22. Zhang, X. H.; Wan, H. M.; Min, Y. Q.; Fang, Z.; Qi, G. R. Chin Chem Lett 2005, 16, 547.
23. Zhang, X. H.; Wan, H. M.; Min, Y. Q.; Qi, G. R. J Appl Polym Sci 2005, 96, 723.
24. Zhang, X. H.; Min, Y. Q.; Wan, H. M.; Qi, G. R. J Appl Polym Sci 2006, 100, 3483.
25. Zhang, X. H.; Chen, S.; Min, Y. Q.; Qi, G. R. Polymer 2006, 47, 1785.
26. Min, Y. Q.; Zhang, X. H.; Zhao, H.; Qi, G. R. Acta Polym Sinica 2006, 7, 855.
27. Zhang, X. H.; Chen, S.; Chen, T.; Sun, X. K.; Liu, F.; Qi, G. R. J Appl Polym Sci 2007, 106, 1632.
28. Zhang, X. H.; Huang, L. H.; Chen, S.; Qi, G. R. Express Polym Lett 2007, 1, 326.
29. Shau, M. D.; Wang, T. S. J Polym Sci Part A: Polym Chem 1996, 34, 387.
30. Espinosa, M. A.; Galia, M.; Cadiz, V. J Polym Sci Part A: Polym Chem 2004, 42, 3516.
31. Lin, C. H. Polymer 2004, 45, 7911.
32. Tarek, A.; Hajime, T.; Tsutomu, T. Polymer 2004, 45, 7903.
33. Sergei, V. L.; Edward, D. W. Polym Int 2004, 53, 1901.
34. Chen, C. S.; Bulkin, B. J.; Pearce, E. M. J Appl Polym Sci 1982, 27, 1177.
35. Iji, M.; Kiuchi, Y. J Mater Sci Mater Electron 2001, 12, 715.
36. Weil, E.; McSwigan, B. J Coat Technol 1994, 66, 75.
37. Schreiber, H.; Saur, W. Makromol Chem Macromol Symp 1993, 74, 165.
38. Horacek, H.; Grabner, W. Makromol Chem Macromol Symp 1993, 74, 271.
39. Hong, X. Y.; Chen, Q. D.; Chen, L.; Chen, M.; Wu, R. G.; Mao, H. Q. Chem J Chin Univ 2002, 23, 744.
40. Hong, X. Y.; Xiao, S. Q.; Chen, Q. L.; Liu, H. W.; Chen, J.; Li, W. T.; Chen, M.; Chen, L. Acta Polym Sinica 2002, 3, 265.
41. Updegraff, I. H. Encyclopedia of Polymer Science and Engineering; Wiley: New York, 1986.
42. Stevens, G.; Richardson, M. Polymer 1983, 24, 851.
43. Doyle, C. D. Anal Chem 1961, 33, 77.
44. Van Krevelen, D. W. Polymer 1975, 16, 615.